



Scaling of Majorana Zero-Bias Conductance Peaks

Fabrizio Nichele,^{1,*} Asbjørn C. C. Drachmann,¹ Alexander M. Whiticar,¹ Eoin C. T. O'Farrell,¹ Henri J. Suominen,¹ Antonio Fornieri,¹ Tian Wang,^{2,3} Geoffrey C. Gardner,^{2,3,4} Candice Thomas,^{2,3} Anthony T. Hatke,^{2,3} Peter Krogstrup,¹ Michael J. Manfra,^{2,4,5,3} Karsten Flensberg,¹ and Charles M. Marcus¹

¹*Center for Quantum Devices and Station Q Copenhagen, Niels Bohr Institute, University of Copenhagen, Universitetsparken 5, 2100 Copenhagen, Denmark*

²*Department of Physics and Astronomy and Station Q Purdue, Purdue University, West Lafayette, Indiana 47907, USA*

³*Birk Nanotechnology Center, Purdue University, West Lafayette, Indiana 47907, USA*

⁴*School of Materials Engineering, Purdue University, West Lafayette, Indiana 47907, USA*

⁵*School of Electrical and Computer Engineering, Purdue University, West Lafayette, Indiana 47907, USA*

(Received 20 June 2017; published 27 September 2017)

We report an experimental study of the scaling of zero-bias conductance peaks compatible with Majorana zero modes as a function of magnetic field, tunnel coupling, and temperature in one-dimensional structures fabricated from an epitaxial semiconductor-superconductor heterostructure. Results are consistent with theory, including a peak conductance that is proportional to tunnel coupling, saturates at $2e^2/h$, decreases as expected with field-dependent gap, and collapses onto a simple scaling function in the dimensionless ratio of temperature and tunnel coupling.

DOI: 10.1103/PhysRevLett.119.136803

Recent years have seen rapid progress in the study of Majorana zero modes (MZMs) in condensed matter. Following initial reports of zero-bias peaks (ZBPs) in conductance of nanowire-superconductor hybrids appearing at moderate magnetic fields [1], improvements in materials [2–4] resulted in harder induced gaps and the emergence of zero-bias peaks from coalescing Andreev bound states (ABSs) [5,6], as well as the observation of exponential suppression of Coulomb peak oscillations with nanowire length [7]. Recently, indications of MZMs were also identified in wires lithographically patterned on hybrid two-dimensional heterostructures [8,9]. In many respects, experimentally observed ZBPs are consistent with theoretical expectations for MZMs, but important questions remain, particularly concerning theoretical models that show ZBPs arising from nontopological ABSs in localized states at the wire ends [10,11]. Furthermore, the fact that observed zero-bias peaks [1,5,6,12] were considerably smaller than the theoretically expected value of $2e^2/h$ [13–18] has raised concern. Speculations about the origin of this discrepancy included effects of dissipation [19] as well as nontopological ZBPs induced by disorder [20–22] or a spin-orbit-induced precursor [10].

In this Letter, we investigate ZBPs in lithographically defined wires as a function of temperature, tunnel coupling to a metallic lead (parametrized by the normal state conductance G_N), and magnetic field. For weak coupling to the lead ($G_N \ll e^2/h$), a small ZBP with strong temperature dependence is observed over an extended range of magnetic fields. For strong coupling ($G_N \sim e^2/h$), the dependence of the ZBP on G_N and temperature weakens, with a low-temperature saturation at $\sim 2e^2/h$. Experimental results are well described by a theoretical model of resonant transport through a

zero-energy state that includes both broadening due to coupling to a normal lead and temperature.

Fitting ZBP heights as a function of temperature, T , and G_N yields values for the energy broadening, Γ , which we find obey the linear relationship $\Gamma \propto G_N$. The fit results for Γ are found to be in excellent agreement with a scaling function that depends only on the dimensionless ratio $\Gamma/k_B T$. The observed magnetic field dependence of the ZBP is quantitatively consistent with a picture wherein the field reduces the induced superconducting gap, Δ^* , which in turn reduces the ZBP height through the dependence of Γ on Δ^* .

Overall, the ZBPs reported here are compatible with MZMs, and suggest that the temperature-to-broadening ratio is the limiting factor controlling ZBP conductance in setups where tunnel coupling is weak [1,6]. We emphasize that although the observed conductance saturation, scaling, and field dependence are all consistent with a MZM interpretation, these results could be obtained with specially tuned nontopological Andreev states that happen to stick to zero energy [11]. Distinguishing topological from trivial scenarios relies on examining the stability of ZBPs to tuning parameters, as discussed below.

Measurements are performed on wires lithographically defined on an InAs/Al heterostructure [8], using the same approach as in Ref. [9]. Figures 1(a) and 1(b) show a schematic and an electron micrograph, respectively, of a typical sample. A 1.5 μm long, 120 nm wide Al strip is defined on the wafer surface by selective Al etching. The Al strip is connected at one end with a large planar Al region, and on the other end terminates with a 40 nm break separating it from another planar Al region. A HfO_2 insulating layer is deposited by atomic layer deposition over the entire sample, followed by two patterned gates

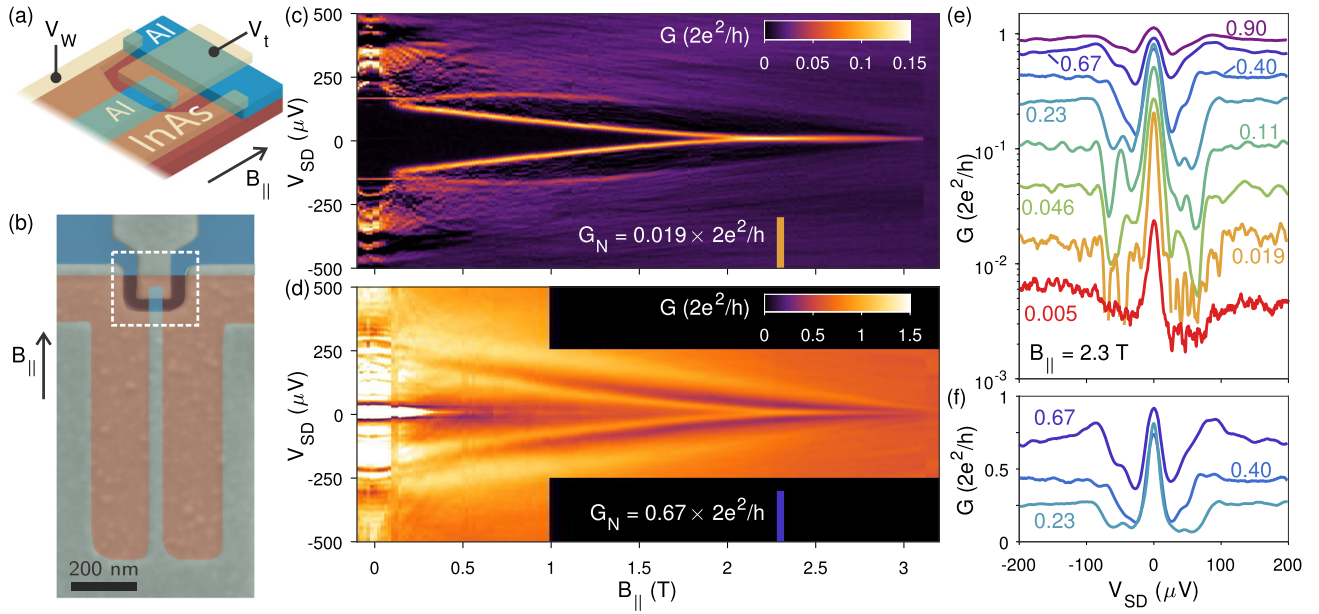


FIG. 1. (a) Device schematic close to the tunneling junction, as in the dashed box in (b). The end of the Al wire and the top Al plane (blue) are separated by a narrow InAs junction (red). Two gates (yellow) allow independent tuning of the chemical potential in the wire (gate voltage V_W) and of the junction transmission (gate voltage V_t). (b) False color scanning electron micrograph of a typical device. The Al pattern is visible through the top gate. The epitaxial Al below the gates is colored gray, the semiconductor below the gates is colored red. (c) Tunneling conductance as a function of in-plane magnetic field B_{\parallel} for normal state transmission $G_N = 0.019 \times 2e^2/h$. The colored line indicates the position where the linecuts of (e) and (f) were taken. Color extrema have been saturated. (d) As in (c) for $G_N = 0.67 \times 2e^2/h$. (e) ZBP conductance at $B_{\parallel} = 2.3$ T for several values of G_N , indicated in the figure in units of $2e^2/h$. (f) Selection of curves from (e), plotted on a linear scale.

separately covering the wire and the break. Applying negative voltage V_W on the gate covering the wire depletes the surrounding two-dimensional electron gas region, leaving a narrow undepleted region of the InAs quantum well screened by the Al strip. The tunnel barrier is independently controlled with the voltage V_t on the break region. Transport measurements are performed using standard low frequency lock-in techniques in a dilution refrigerator with base electron temperature of ~ 40 mK. Throughout this paper, we characterize the low-temperature transport measurements in terms of the normal state conductance, G_N , measured as the differential conductance at large source drain bias V_{SD} . These values coincide with the $V_{SD} = 0$ conductances measured above the critical temperature of the Al film. Further details of wafer structure, sample fabrication, as well as additional measurements are given in the Supplemental Material [23].

For magnetic fields B_{\parallel} (oriented along the wire) lower than ~ 100 mT, both the strip and plane regions of the quantum well covered by Al show a hard induced superconducting gap, resulting in a superconductor-insulator-superconductor (SIS) junction. At larger fields, the superconducting gap below the Al plane softens, creating a finite density of state at zero energy, while the gap below the Al strip remains hard up to 3 T [9]. This feature allows the Al plane to be used, at moderate B_{\parallel} , as an

effective normal lead, making a superconductor-insulator-normal (SIN) junction, which can be used to perform tunneling spectroscopy of the wire.

Tunneling conductance as a function of B_{\parallel} at small and large barrier transmissions (controlled by V_t) for similar wire densities (controlled by V_W) are shown in Figs. 1(c) and 1(d). For large transmission and low field, the SIS configuration is evident from a conductance enhancement at $V_{SD} = 0$ [up to $100 \times 2e^2/h$ in the data of Fig. 1(d)] as well as tunneling conductance peaks at $V_{SD} = \pm 2\Delta^*/e \sim \pm 400 \mu\text{V}$ and fractions reflecting multiple Andreev reflection [24,25]. The zero bias supercurrent disappears as the transmission is lowered, while low-order multiple Andreev reflections remain. In Fig. 1(d), for example, the first order Andreev reflection is visible as a conductance peak at $V_{SD} = \pm \Delta^*/e \sim \pm 200 \mu\text{V}$. Regardless of transmission, the planar lead acquires effectively normal behavior above $B_{\parallel} \sim 300$ mT, as seen from the crossover of tunneling features from $\pm 2\Delta^*/e$ (expected for SIS) to $\pm \Delta^*/e$ (expected for SIN).

At larger fields, $B_{\parallel} \sim 2$ T, a robust ZBP forms from subgap states moving toward zero energy. While the overall appearance of data in Fig. 1(c) suggests a MZM interpretation, an explanation in terms of localized Andreev bound states that happen to stick to zero energy [11] cannot be ruled out by these measurements alone. Further support for

a MZM interpretation includes field-angle and gate dependence (see Figs. S1-2 in Ref. [23]), rehardening of the gap at high field (see Fig. S3 in Ref. [23]), as well as stability of the ZBP with respect to gate voltages applied close to the lithographic end of the wire, as discussed in reference to Fig. 4.

The same ZBP was measured for tunnel couplings ranging from $G_N = 0.005 \times 2e^2/h$ to $1 \times 2e^2/h$, by tuning V_i . For low transmission, a sharp ZBP was observed on a hard gap, as seen in Fig. 1(c). The peak height, G_P , defined as the conductance at $V_{SD} = 0$ without background subtraction, was up to 10 times higher than G_N , though still considerably lower than $2e^2/h$. Increasing G_N by adjusting V_i broadened the peak and increased G_P toward $\sim 2e^2/h$, while decreasing the ratio G_P/G_N toward 1. The linear vertical scale in Fig. 1(f) emphasizes that as G_N increased by a factor of nearly 3, from 0.23 to 0.67 in units of $2e^2/h$, the ZBP height only changed by about 10%. Additionally, G_P is found to decrease as B_{\parallel} increases, an effect we attribute to the collapsing gap, as discussed below.

Increasing the tunnel coupling not only increased G_P , but also increased the background subgap conductance, as expected theoretically [24,26]. Large magnetic fields further soften the superconducting gap [3,27]. For $G_N = 0.23 \times 2e^2/h$, the zero bias conductance peak is $G_P = 0.81 \times 2e^2/h$, 12 times higher than the conductance minimum at finite V_{SD} , below the gap edge [see Figs. 1(e) and 1(f)]. As the barrier transmission is further increased, the contribution from the ZBP is no longer well separated from the above-gap conductance. The analysis of the dependence of G_P on transmission presented below suggests that more than one channel participates in the transport. This presumably also accounts for the low-temperature saturation of G_P for the most open barrier exceeding $2e^2/h$ by $\sim 13\%$. A ZBP is not visible for G_N above $2e^2/h$.

Turning next to the temperature dependence of ZBPs at different tunnel couplings, Figs. 2(a) and 2(b) show cuts from Figs. 1(c) and 1(d) at $B_{\parallel} = 2.3$ T, for temperatures ranging from 40 to 600 mK. In both cases, reducing the temperature results in an increase of the ZBP height and a reduction of its width. The temperature dependence of the ZBP height depends on transmission: lowering T from 60 to 40 mK increases G_P at low transmission by 90% [Fig. 2(a)], while G_P at high transmission increases by only 15% [Fig. 2(b)]. Temperature dependence across a broad range of transmissions is shown in Fig. 2(c). Consistent with the examples in Figs. 2(a) and 2(b), values of G_P in Fig. 2(c) depend only weakly on T for high transmission, near $G_P \sim 2e^2/h$, while for low transmission, G_P values depend strongly on temperature.

These observations can be compared to a model of a MZM broadened by tunnel coupling and temperature. For energies below the topological gap Δ_t , tunnel broadening gives a Lorentzian line shape to the zero-temperature

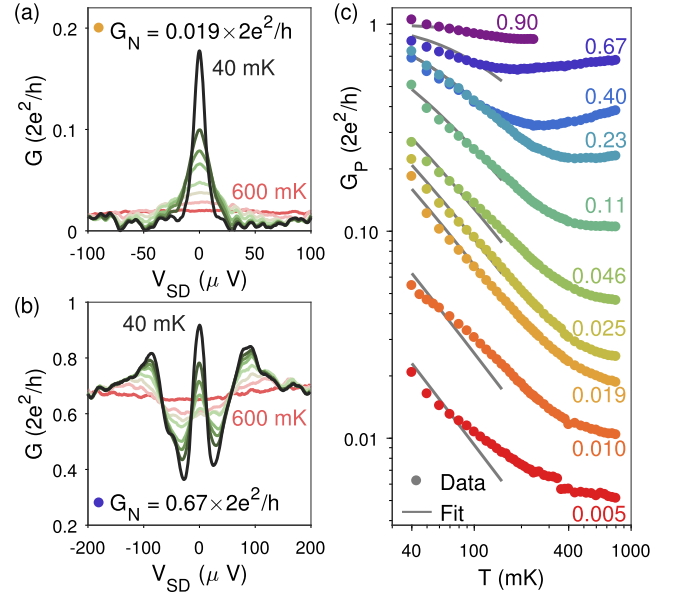


FIG. 2. (a) Conductance of a ZBP at $B_{\parallel} = 2.3$ T and $G_N = 0.19 \times 2e^2/h$ for various temperatures. Temperatures are 40 (black), 60, 80, 100, 150, 200, 300, and 600 mK (pink). (b) As in (a), but for $G_N = 0.67 \times 2e^2/h$. (c) Temperature dependence ZBP conductance, G_P , at $B_{\parallel} = 2.3$ T, measured for different values of G_N (colored dots) together with fits to Eq. (1) (gray curves). For the experimental data, the same colors as in Fig. 1(e) are used.

Majorana peak [13,16,18,28]. For weak tunneling, the width, Γ , of the ZBP is predicted to be directly proportional to the transparency τ of the junction and the topological gap, $\Gamma \propto \tau \Delta_t$ [13,18,28]. Physically, the proportionality to the gap reflects the tighter localization of the MZM to the boundary of the topological region with larger gap. According to this picture, for $k_B T \ll \Delta_t$ the zero-bias conductance is given by

$$G_P \approx \frac{e^2}{h} \int_{-\infty}^{\infty} d\omega \frac{2\Gamma^2}{\omega^2 + \Gamma^2} \frac{1}{4k_B T \cosh^2(\omega/(2k_B T))} = \frac{2e^2}{h} f(k_B T/\Gamma). \quad (1)$$

Note that the scaling function f depends only on the ratio of temperature to tunnel broadening. Fits of Eq. (1) to the $T \leq 150$ mK data in Fig. 2(c) yield values for the single fit parameter Γ for each value of G_N . The resulting values are shown in Fig. 3(a). The fit values of Γ were found to be proportional to G_N [gray line in Fig. 3(a)] over 2 orders of magnitude. A power-law fit of the form $\Gamma \propto (G_N)^\alpha$ yields $\alpha = 1.0 \pm 0.1$.

A spinless model for MZM transport yields the relation $\Gamma = \tau \Delta_t / (2\sqrt{1-\tau})$ across the full range of transmission $0 < \tau < 1$ [13,29]. On the other hand, experimentally, we find that the linear relation $\Gamma \propto G_N$ holds even as

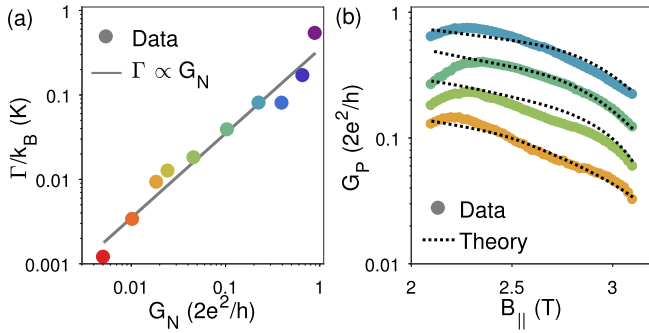


FIG. 3. (a) Extracted relation between the tunnel broadening, Γ , obtained from the fits in Fig. 2(c), and the normal-state conductance, G_N (dots), along with a linear fit (gray line). (b) Magnetic field dependence of the ZBP conductance, G_P , together with theoretical predictions based on Eq. (1), with $\Gamma \propto \Delta^*(B_{||})$.

$G_N \rightarrow 2e^2/h$ [Fig. 3(a)], apparently inconsistent with the spinless model if one makes the identification $\tau = G_N/(2e^2/h)$. We note, however, that the spinless model is not valid for Γ of order the gap. A spinful single-mode model with transmission close to unity predicts an in-gap conductance near $4e^2/h$ at finite bias, with a dip rather than a peak at zero bias to $2e^2/h$ [17,30], which we do not observe. Conductance doubling due to Andreev reflection was recently observed by us in a different device geometry [27], but only at low field and zero bias. A hint to this behavior might be visible in the highest transmission curves of Fig. 1(e), where the finite bias in-gap conductance quickly raises as transmission approaches unity. These discrepancies between model predictions and experiment could also suggest that more transverse modes below the Al strip contribute to transport. A multimode scenario could also explain the observation of G_P exceeding $2e^2/h$ when $G_N \sim 2e^2/h$, as seen in Fig. 2(c) (violet dots) while still being in agreement with the small conductance traces, keeping in mind that the contribution to Andreev reflection from the additional modes would not significantly modify the low temperature quantization for $\tau \ll 1$ [24,26]. These observations motivate a more detailed understanding of the finite-bias transport in multimode topological wires.

The linear fit in Fig. 3(a) gives $\Gamma/k_B \sim G_N/(2e^2/h) \times 430 \text{ mK}$. With $\tau = G_N/(2e^2/h)$, the model relation $\Gamma \approx \tau \Delta_t/2$ (valid for $\tau \ll 1$) yields $\Delta_t \sim 75 \mu\text{eV}$, which is comparable to the gap measured directly from Figs. 1(c)–1(f). The proportionality $\Gamma \propto \Delta_t$ suggests a mechanism for the observed reduction of the ZBP as $B_{||}$ increases: quenching of Δ_t by the external field reduces Γ , which in turn lowers G_P through the ratio $k_B T/\Gamma$ [see Eq. (1) and Fig. 4]. To test this connection quantitatively, we used $\Delta^*(B_{||})$ from various measurements including data in Figs. 1(c) and 1(d) to calculate G_P , assuming $\Gamma(B_{||}) = \tau \Delta^*(B_{||})/2$ and Eq. (1). Figure 3(b) shows good agreement between experiment and this simple calculation, indicating that the reduction of the ZBP at high field is a consequence of the closing of the

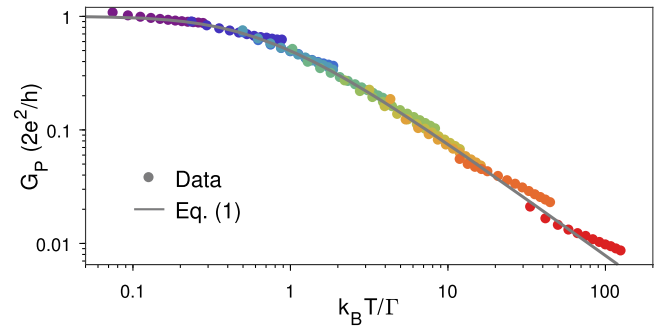


FIG. 4. Zero bias conductance of the entire data set (for $T \leq 150 \text{ mK}$) plotted as a function of temperature scaled by the extracted values of Γ (colored dots) and compared to the theoretical expectation of Eq. (1) (gray curve).

induced gap [31]. We note that the observed decrease in ZBP height with decreasing $\Delta^*(B_{||})$ suggests a mode fixed to the end of the wire. In contrast, for a mode away from the end of the wire (on the scale of a coherence length) an increase in tunnel coupling as $\Delta^*(B_{||})$ decreases would be expected.

Zero-bias peak conductances for the full range of the dimensionless scale factor $k_B T/\Gamma$ are shown in Fig. 4 along with the scaling function, Eq. (1), for transport through a single zero-energy mode. A striking consistency over 3 orders of magnitude in $k_B T/\Gamma$, with low-temperature saturation $2e^2/h$, is observed. We emphasize that scaling and saturation at $2e^2/h$, as expected for a MZM, does not rule out a nontopological discrete state at zero energy, for instance of the type discussed in Ref. [11], as the origin of the ZBP. Support for a MZM interpretation includes the robustness of features to variation in $B_{||}$, V_W , and V_t . We found that gate voltage V_t tunes the tunneling probe transmission up to 3 orders of magnitude but does not affect the ZBP except for the behavior captured by Eq. (1). A disorder-induced bound state near the end of our wires would presumably be affected by V_t [see Fig. 1(a)], resulting in variations of occupation, low temperature conductance, and behavior in a magnetic field. Essentially identical behavior seen in a second device [23] further suggests a MZM rather than a localized state resulting from disorder.

A similar single parameter scaling has been applied to Kondo resonances in quantum dots [32], including devices with superconducting leads [33]. Qualitatively similar to Fig. 4, the Kondo resonance results in a ZBP with low temperature saturation to $2e^2/h$ and a suppression at high temperature, despite a different functional form than Eq. (1). The emergence of the ZBP from Andreev states converging at zero energy disfavors a Kondo interpretation. Also, the Kondo resonance typically requires low magnetic fields and symmetric leads. Here we operate in a very large field and with a single tunnel barrier whose transmission is tuned by more than 2 orders of magnitude without affecting the presence of the ZBP.

In conclusion, we have investigated ZBPs in a Majorana device patterned in a two-dimensional heterostructure with epitaxial Al. The devices design allows a systematic study of the conductance for different values of the tunnel broadening. The low-temperature data show a scaling behavior where the peak height follows a simple universal curve that depends only on the dimensionless parameter $k_B T/\Gamma$ and saturates at $2e^2/h$ for $k_B T/\Gamma \ll 1$. These results suggest that small ZBPs previously reported may be compatible with MZMs if they were obtained in a regime where the ratio of temperature to broadening was large.

This work was supported by Microsoft Corporation, the Danish National Research Foundation, the Villum Foundation, and the DFG Mercator program. We thank Joshua Folk and Michael Hell for useful discussions.

*fnichele@nbi.ku.dk

- [1] V. Mourik, K. Zuo, S. M. Frolov, S. R. Plissard, E. P. A. M. Bakkers, and L. P. Kouwenhoven, *Science* **336**, 1003 (2012).
- [2] P. Krogstrup, N. L. B. Ziino, W. Chang, S. M. Albrecht, M. H. Madsen, E. Johnson, J. Nygård, C. M. Marcus, and T. S. Jespersen, *Nat. Mater.* **14**, 400 (2015).
- [3] W. Chang, S. M. Albrecht, T. S. Jespersen, F. Kuemmeth, P. Krogstrup, J. Nygård, and C. M. Marcus, *Nat. Nanotechnol.* **10**, 232 (2015).
- [4] O. Gül, H. Zhang, F. K. de Vries, J. van Veen, K. Zuo, V. Mourik, S. Conesa-Boj, M. P. Nowak, D. J. van Woerkom, M. Quintero-Perez, M. C. Cassidy, A. Geresdi, S. Koelling, D. Car, S. R. Plissard, E. P. A. M. Bakkers, and L. P. Kouwenhoven, *Nano Lett.* **17**, 2690 (2017).
- [5] H. Zhang, Ö. Gül, S. Conesa-Boj, K. Zuo, V. Mourik, F. K. de Vries, J. van Veen, D. J. van Woerkom, M. P. Nowak, M. Wimmer, D. Car, S. Plissard, E. P. A. M. Bakkers, M. Quintero-Pérez, S. Goswami, K. Watanabe, T. Taniguchi, and L. P. Kouwenhoven, *arXiv:1603.04069*.
- [6] M. T. Deng, S. Vaitiekenas, E. B. Hansen, J. Danon, M. Leijnse, K. Flensberg, J. Nygård, P. Krogstrup, and C. M. Marcus, *Science* **354**, 1557 (2016).
- [7] S. M. Albrecht, A. P. Higginbotham, M. Madsen, F. Kuemmeth, T. S. Jespersen, J. Nygård, P. Krogstrup, and C. M. Marcus, *Nature (London)* **531**, 206 (2016).
- [8] J. Shabani, M. Kjaergaard, H. J. Suominen, Y. Kim, F. Nichele, K. Pakrouski, T. Stankevic, R. M. Lutchyn, P. Krogstrup, R. Feidenhans'l, S. Kraemer, C. Nayak, M. Troyer, C. M. Marcus, and C. J. Palmstrøm, *Phys. Rev. B* **93**, 155402 (2016).
- [9] H. J. Suominen, M. Kjaergaard, A. R. Hamilton, J. Shabani, C. J. Palmstrøm, C. M. Marcus, and F. Nichele, *arXiv:1703.03699*.
- [10] E. J. H. Lee, X. Jiang, M. Houzet, R. Aguado, C. M. Lieber, and S. De Franceschi, *Nat. Nanotechnol.* **9**, 79 (2013).
- [11] C.-X. Liu, J. D. Sau, T. D. Stanescu, and S. Das Sarma, *Phys. Rev. B* **96**, 075161 (2017).
- [12] A. Das, Y. Ronen, Y. Most, Y. Oreg, M. Heiblum, and H. Shtrikman, *Nat. Phys.* **8**, 887 (2012).
- [13] K. Sengupta, I. Žutić, H.-J. Kwon, V. M. Yakovenko, and S. Das Sarma, *Phys. Rev. B* **63**, 144531 (2001).
- [14] K. T. Law, P. A. Lee, and T. K. Ng, *Phys. Rev. Lett.* **103**, 237001 (2009).
- [15] A. R. Akhmerov, J. Nilsson, and C. W. J. Beenakker, *Phys. Rev. Lett.* **102**, 216404 (2009).
- [16] K. Flensberg, *Phys. Rev. B* **82**, 180516 (2010).
- [17] M. Wimmer, A. R. Akhmerov, J. P. Dahlhaus, and C. W. J. Beenakker, *New J. Phys.* **13**, 053016 (2011).
- [18] A. Zazunov, R. Egger, and A. Levy Yeyati, *Phys. Rev. B* **94**, 014502 (2016).
- [19] C.-X. Liu, J. D. Sau, and S. Das Sarma, *Phys. Rev. B* **95**, 054502 (2017).
- [20] J. Liu, A. C. Potter, K. T. Law, and P. A. Lee, *Phys. Rev. Lett.* **109**, 267002 (2012).
- [21] D. Bagrets and A. Altland, *Phys. Rev. Lett.* **109**, 227005 (2012).
- [22] D. I. Pikulin, J. P. Dahlhaus, M. Wimmer, H. Schomerus, and C. W. J. Beenakker, *New J. Phys.* **14**, 125011 (2012).
- [23] See Supplemental Material at <http://link.aps.org/supplemental/10.1103/PhysRevLett.119.136803> for material and methods and additional measurements.
- [24] G. E. Blonder, M. Tinkham, and T. M. Klapwijk, *Phys. Rev. B* **25**, 4515 (1982).
- [25] M. Kjaergaard, H. J. Suominen, M. P. Nowak, A. R. Akhmerov, J. Shabani, C. J. Palmstrøm, F. Nichele, and C. M. Marcus, *Phys. Rev. Applied* **7**, 034029 (2017).
- [26] C. W. J. Beenakker, *Phys. Rev. B* **46**, 12841 (1992).
- [27] M. Kjaergaard, F. Nichele, H. J. Suominen, M. P. Nowak, M. Wimmer, A. R. Akhmerov, J. A. Folk, K. Flensberg, J. Shabani, C. J. Palmstrøm, and C. M. Marcus, *Nat. Commun.* **7**, 12841 (2016).
- [28] B. van Heck, R. M. Lutchyn, and L. I. Glazman, *Phys. Rev. B* **93**, 235431 (2016).
- [29] S. Kashiwaya and Y. Tanaka, *Rep. Prog. Phys.* **63**, 1641 (2000).
- [30] F. Setiawan, P. M. R. Brydon, J. D. Sau, and S. Das Sarma, *Phys. Rev. B* **91**, 214513 (2015).
- [31] The theory curves are calculated for $T = 55$ mK due to the elevated electron temperature during magnetic field sweeps [23].
- [32] W. G. van der Wiel, S. D. Franceschi, T. Fujisawa, J. M. Elzerman, S. Tarucha, and L. P. Kouwenhoven, *Science* **289**, 2105 (2000).
- [33] E. J. H. Lee, X. Jiang, R. Aguado, G. Katsaros, C. M. Lieber, and S. De Franceschi, *Phys. Rev. Lett.* **109**, 186802 (2012).